

CD12: a new high-flux beamline for ultra-violet and vacuum-ultraviolet circular dichroism on the SRS, Daresbury

David Thomas Clarke* and Gareth Jones

CCLRC Daresbury Laboratory, Daresbury, Warrington WA4 4AD, UK. E-mail: d.t.clarke@dl.ac.uk

This paper describes the commissioning and characterization of an SRS bending-magnet beamline constructed for the measurement of vacuum-ultraviolet circular dichroism on biological and other materials. The beamline provides photon fluxes of many orders of magnitude greater than commercial instruments or beamlines at other synchrotron radiation facilities. The beamline uses the conventional approach of utilizing the plane polarized light emitted from the bending magnet which is subsequently converted into circularly polarized light using a photoelastic modulator with a switching frequency of 50 kHz. The beamline has a best wavelength resolution of 0.5 nm and stray light levels better than 0.01%. The latter may be predicted to give improved performance over other beamlines at synchrotron radiation sources especially when short-wavelength CD spectra are to be collected. An example spectrum and submillisecond time-resolved CD profile are given and the impact that the new beamline is likely to have is speculated on. The ultimate flux limitations of the technique with regard to the avoidance of the effects of radiation damage are also discussed.

Keywords: circular dichroism; protein secondary structure; vacuum-ultraviolet spectroscopy.

1. Introduction

Circular dichroism (CD) spectroscopy measures the difference in absorption between left and right circularly polarized light by a chiral molecule (Rodger & Nordén, 1997). CD provides structural information on biological macromolecules such as proteins, nucleic acids and carbohydrates because the chirality of the amino acids and sugars that are the 'building blocks' of the molecules confers handedness to their backbone structure (Jones & Munro, 2000). CD has been applied extensively to the investigation of the structure of proteins, in particular the secondary structure, which describes how the polypeptide chain is folded into structural forms such as alpha helices and beta sheets. The ultraviolet and vacuum-ultraviolet (UV-VUV) region of the spectrum, between around 150 and 260 nm, reports on protein secondary structure, each structure type having a characteristic CD signature (Fasman, 1996). Ever-increasing protein structure information is becoming available from the Protein Data Bank (Berman *et al.*, 2000), and there are a number of programs available to obtain secondary structure content from the atomic coordinates (Frishman & Argos, 1995). This, together with software and associated web servers for extracting secondary structure from CD data (Lobley *et al.*, 2002; Greenfield, 1996), means that CD is being employed more frequently as a structural biology technique.

CD measurements are fast and simple, requiring no extensive sample preparation, and a secondary structure analysis can be performed in a matter of seconds. Measurements are usually performed in the solution phase, and require relatively small amounts of sample, which may be any size of macromolecule. Time-resolved CD measurements are also possible, in the millisecond regime using

conventional techniques (Kuwanjima, 1996), and with pico/nano-second resolution using ellipsometry (Goldbeck *et al.*, 1997). For these reasons, CD is often used to complement the more detailed structural information available from other techniques such as X-ray crystallography and NMR spectroscopy.

CD measurements can be made effectively using conventional instruments equipped with xenon lamps. However, these suffer from a number of disadvantages, particularly their low photon fluxes in the sub-190 nm region of the spectrum. Significant improvements in secondary structure analysis can be made if protein spectra can be extended into this region (Johnson, 1996; Jones & Clarke, 2003), and the CD bands of carbohydrates are found almost entirely in the VUV region (Stevens, 1996). Synchrotron radiation has for some time been considered an excellent source for CD measurements; it is inherently linearly polarized in the plane of the ring making it highly suitable to be converted to left- and right-handed circularly polarized light, and VUV fluxes are high. The use of synchrotron radiation for UV and VUV CD was first described over 20 years ago (Sutherland *et al.*, 1980; Snyder & Rowe, 1980). Synchrotron radiation CD (SRCD) has since been provided for by a number of facilities, including the SRS, but measurements are generally made on general-purpose VUV spectroscopy beamlines not optimized for the specific requirement of CD (Clarke & Jones, 1999; Clarke *et al.*, 1999; Sutherland *et al.*, 1992). However, the quality of the data reported has demonstrated the superiority of synchrotron radiation as a CD source.

To provide a beamline optimized for CD a number of essential specifications were considered at the design stage. Firstly, tunability and high flux in the wavelength region from 120 to 300 nm initially, with the option for extending this into the visible and near-infrared regions. Secondly, a high degree of stable linear polarization, and thirdly, low levels of stray light. Spectral resolution requirements are modest at around 0.5 nm. There was also a requirement to be able to select specific portions of the synchrotron radiation beam for control over the degree of linear polarization. Here we describe performance tests of CD12 and show test data confirming its high performance for the measurement of SRCD.

2. Beamline description

CD12 has been designed for optimal performance for CD measurements in the wavelength range from 120 to 1000 nm. A photoelastic modulator (Hinds International PEM-90) (Kemp, 1969) generates switched left- and right-handed circularly polarized light without the necessity of having to employ a polarizing optic because of the inherent linear polarization of the synchrotron light. The general layout and components of CD12 are shown in Fig. 1. The beamline consists of a front end with defining apertures and beam-position monitor, a vertically deflecting plane mirror, pre-monochromator beam-defining baffles, a toroidal grating monochromator, post-monochromator baffles, an acoustic delay line, exit slits and an end window.

2.1. Front end

CD12 is installed on bending-magnet 12 of the SRS. The main components of the front end are the water-cooled beam absorber, defining apertures, two vacuum valves and a motorized scanning tungsten vane monitor for measurement of beam position. The apertures accept almost all of the UV radiation from the bending magnet (35 mrad horizontal, 7 mrad vertical).

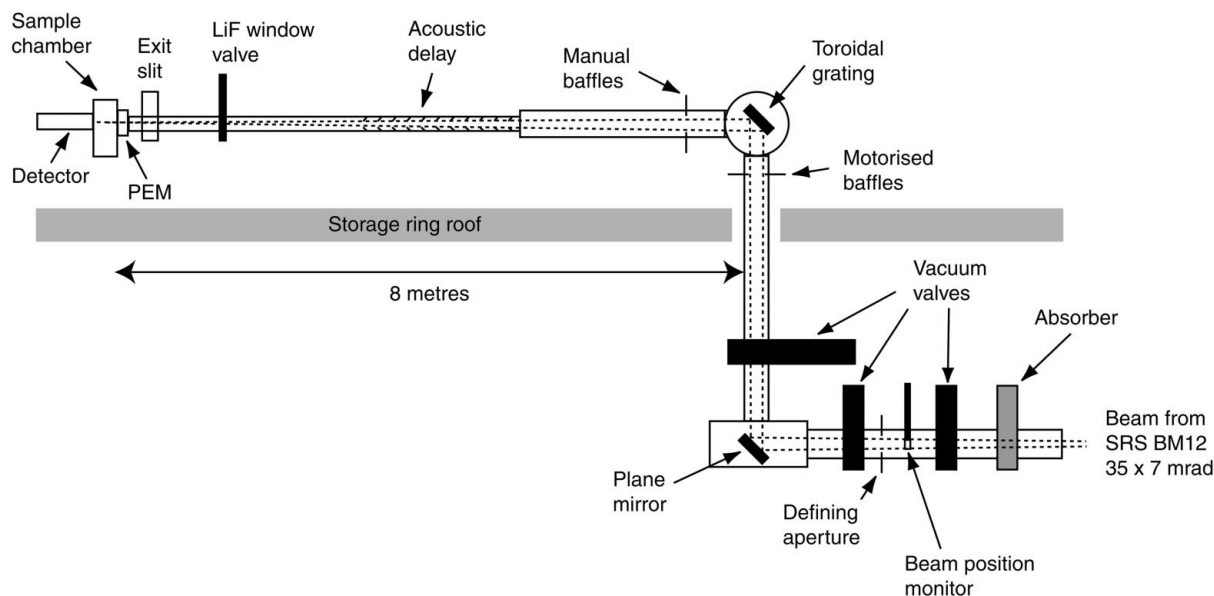


Figure 1
Layout of CD12 showing the major components.

2.2. Mirror

Space constraints around bending-magnet 12 require that the beamline is located on the roof of the storage ring. The mirror is planar, deflecting the beam upwards at 90° . The substrate material is silicon, with a coating of aluminium. Cooling is provided by the circulation of water through copper blocks clamped to the sides of the mirror with a conducting interface of indium foil. Finite-element analysis has shown this type of cooling to minimize slope errors due to heating of the mirror by the X-ray component of the beam. Motor drives are used to adjust the mirror roll and tilt.

2.3. Beam-defining baffles

Baffles have been incorporated into the beamline for two reasons. Firstly, to minimize the stray light component at the detector. Secondly, to allow control of the part of the beam selected, to optimize the degree of polarization characteristics of the beam. Each set of baffles consists of four independently adjustable blades (two vertical, two horizontal). When used in combination, these baffles allow any part of the beam to be selected. The pre-monochromator baffles are motor-driven, while the post-monochromator baffles are manually operated.

2.4. Monochromator

The monochromator and grating were manufactured by Jobin Yvon SAS (Longjumeau, France). The monochromator has the facility to hold up to three diffraction gratings or mirrors simultaneously. Because of the beamline geometry and large acceptance angle of the front end, the optical elements are large ($300\text{ mm} \times 80\text{ mm} \times 80\text{ mm}$). The size and weight of the gratings required careful design of the mechanism to achieve the design wavelength resolution and positional repeatability (minimum wavelength step = 0.1 \AA). The grating carriage is mounted on a wheel, supported on three bearings. Wavelength is selected by rotating the wheel, which is pushed by a sine arm, motorized through a lead screw. The motor, gearbox and lead screw pitch arrangement finalized on gave $1\text{ }\mu\text{m}$ of linear movement for every motor step. Grating yaw and roll are adjustable manually through vacuum feedthroughs. At present, only one optical element is installed. This is a toroidal diffraction grating, designed for

Table 1

Specifications of the CD12 diffraction grating.

Grating profile	Lamellar
Production process	Holographically recorded, ion-beam etched
Substrate	Fused silica
Coating	Aluminium
Coating thickness	$400 \pm 40\text{ \AA}$
Line density	$300 \pm 1\text{ lines mm}^{-1}$
Line density uniformity	± 0.02
Groove width	$17000 \pm 500\text{ \AA}$
Groove depth	$725 \pm 50\text{ \AA}$
Major radius (tangential)	$10.42 \pm 0.02\text{ m}$
Minor radius (sagittal)	$5.302 \pm 0.01\text{ m}$

peak output around 200 nm . The specifications of the grating are shown in Table 1. The grating radii were selected to give vertical focusing at the exit slit (7.8 m from the monochromator), and horizontal focusing at the sample position (0.2 m from the exit slit), at a wavelength of 200 nm . This configuration results in a horizontal beam size of 5 mm at the sample. The vertical beam size depends on the slit setting, and is around 2 mm for a 0.5 nm bandpass. The beam size at the sample position does not change significantly throughout the wavelength range used for CD spectroscopy with the installed grating ($130\text{--}280\text{ nm}$).

2.5. Exit slit

The exit slits were also manufactured by Jobin Yvon. A lead screw driven by a stepper motor pushes a wedge which determines the slit width. The slit width is adjustable from a nominal zero ($2\text{ }\mu\text{m}$ to prevent the slits coming into contact with each other) to 10 mm . One motor step corresponds to a change in width of $2\text{ }\mu\text{m}$. The slits are chamfered at an angle of 45° to minimize scatter.

2.6. Sample environment

The sample environment was designed for maximum flexibility, and consists of an optical table placed at the end of the beamline, after the lithium fluoride exit window. For CD measurements, a photoelastic modulator (Hinds Instruments PEM-90) is located in a light-tight nitrogen-purged chamber mounted on the optical table. As

PEMs are calibrated using helium neon lasers at a wavelength of 632.8 nm, additional calibration for the VUV region was made by optimizing the PEM retardation setting to maximize the CD signal at 192.5 nm from a solution of (1*s*)-(+)-10-camphorsulphonic acid. A more extensive calibration procedure, using a crossed-polarizer technique previously employed on other synchrotron sources (Oakberg *et al.*, 2000) is currently in progress for the PEMs in use on CD12.

The sample stage is housed in a second nitrogen-purged chamber. The stage for scanning CD measurements consists of a copper block, which is temperature-controlled by Peltier heat pumps. Control of temperature is available through the data-acquisition program. For time-resolved CD measurements, other devices such as a stopped-flow apparatus can replace this sample stage.

2.7. Data-acquisition system

Fig. 2 shows a schematic diagram of the data-acquisition electronics for scanning CD. The concept is the same as that employed in conventional CD instruments and on other synchrotron CD stations (Sutherland, 1996). A photomultiplier tube (PMT) detects the signal. Normally a solar blind PMT is used (Electron Tubes 9402B), but other detectors can be used for measurements in the visible region. After amplification, the signal is separated into its AC and DC components in the signal-conditioning unit (Hinds SCU-90). The PMT HT servo unit adjusts the bias HT on the detector to maintain the DC component of the signal constant, irrespective of sample absorbance and light output from the station. Because the DC level is kept constant, the AC signal is directly proportional to the CD signal. This signal is detected by a lock-in amplifier (Signal Recovery 5209), using the modulation frequency of the PEM as a reference. A voltage-to-frequency converter is used to convert the output from the lock-in amplifier to a frequency signal, which is recorded using a PC with counter/timer card (National Instruments PCI-6602). Other signals, such as photomultiplier HT and storage-ring current, can also be recorded in the same way.

3. Measurements of station performance

Station performance was assessed according to a series of criteria, as described below. Absorbance measurements were made by recording photomultiplier currents with constant HT in the presence (*I*) and absence (*I*₀) of sample, and absorbance (*A*) calculated from the equation $A = \log(I_0/I)$.

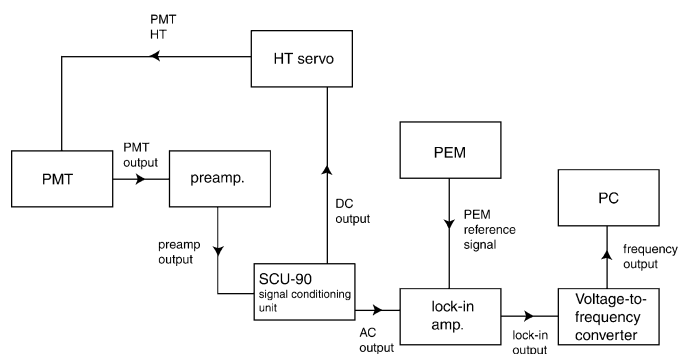


Figure 2
Block diagram of CD12 PMT high-tension control servo, signal processing and data-acquisition system.

3.1. Photon flux

The photon flux was measured using a calibrated photomultiplier tube (Electron Tubes 9402B), mounted in the beamline after the exit slit. The photon flux is shown in Fig. 3. For comparison, photon fluxes from SRS stations previously used for CD, and from a conventional CD instrument, are also shown. At 200 nm, the flux from CD12 is almost five orders of magnitude greater than the conventional instrument, and four orders greater than the former SRS CD station 3.1, which typically achieved maximum photon fluxes around 10^{10} photons s^{-1} with recently cleaned optical elements. Below 200 nm, the advantages of 3.1 over conventional instruments become more significant, and the quality of our early data from this station (Clarke & Jones, 1999) prompted the successful funding application for CD12.

3.2. Wavelength resolution

The resolution was determined by measuring the absorbance of a calibrated sample of 0.02% toluene in hexane (Optiglass Ltd). Absorbance scans were recorded over the absorbance minimum at around 268.7 nm, and the maximum at around 270 nm, at a range of exit slit settings (Fig. 4). The resolution was determined from the ratio of absorbance maximum to absorbance minimum. The measurements show an achievable resolution range of 0.5 to 2.0 nm, meeting the design specification.

3.3. Wavelength calibration and stability

The wavelength was calibrated by measuring the absorbance of a reference solution of 4% holmium oxide in 10% perchloric acid (Optiglass Ltd). Holmium peak positions were used to calibrate the monochromator ratio of motor steps to wavelength change. Data from this calibration scan are shown in Fig. 5. Over the wavelength range scanned, all the holmium absorbance maxima were within 0.1 nm of the correct value. Stability of the wavelength calibration was checked by a series of scans taken before and after storage-ring refills (Fig. 6). At the two maxima measured, wavelength calibration was stable to within 0.1 nm for the duration of the measurements. Longer-term measurements (not shown) have confirmed that wavelength calibration remained reproducible to the 0.1 nm level for all of

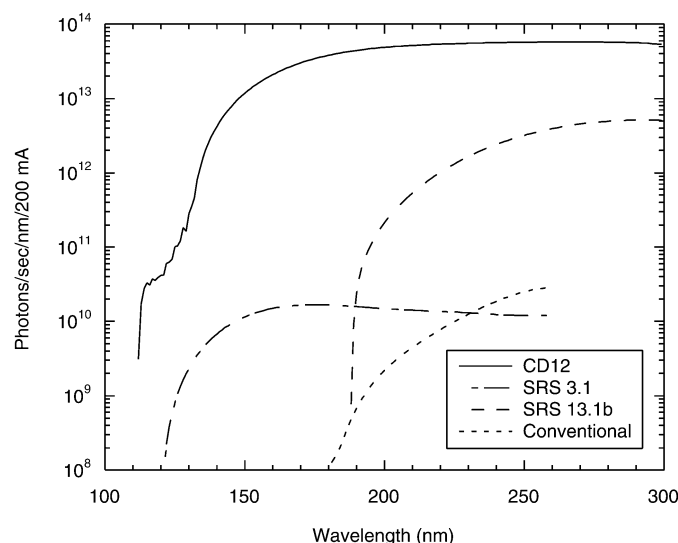


Figure 3
Photon flux from CD12 compared with flux from a conventional instrument and SRS beamlines used for CD measurements.

the station commissioning programme (approximately one month). Again, this stability is well within the specified level.

3.4. Stray light

Stray light levels were measured by recording the transmission of a series of calibrated solutions of potassium chloride (1.2%), sodium iodide (1%) and lithium carbonate (saturated) (Optiglass Ltd). These scans are shown in Fig. 7. Absorbance cut-offs for these materials are 200, 227 and 260 nm, respectively. The measurements show stray light to be between 0.01% at 180 nm and 0.005% at 240 nm, consistent with the angular distance of the grating from zero order where all wavelengths are transmitted. The measurement of CD spectra demands low levels of stray light because of the manner in which the PMT HT is servoed to maintain a constant current output during the acquisition of a spectrum. In the VUV where the sample absorbance

is high the system responds by applying high PMT HTs and the detector becomes very sensitive to low levels of stray light. If the level of stray light is such that it is measured by the detector, at wavelengths where a CD signal cannot be detected due to the high absorbance of the sample, then a spurious signal will be recorded. The levels of stray light measured on CD12 are within design specification and considered to be acceptable for SRCD measurements.

3.5. Polarization

The polarization of the CD12 beam was measured using an Instrument Systems RPA 2000 polarization analyser. This device uses a rotating waveplate to measure the Stokes parameters. Fig. 8 shows the polarization ellipse, azimuth and degree of linear polarization measured over a 6 h period, at 200 nm wavelength, resolution of 1 nm. Both the ellipticity and the azimuth were close to the desired zero level, with a maximum drift over the 6 h measurement period of 0.15° for both parameters. The degree of linear polarization was

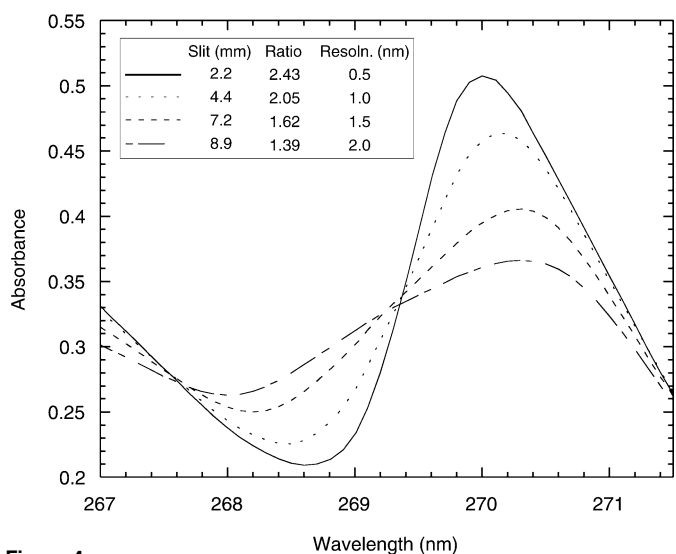


Figure 4 Absorbance spectra of toluene in hexane recorded on CD12 at a range of slit widths. The ratio between the maximum around 270 nm and the minimum around 268.7 nm measures spectral resolution.

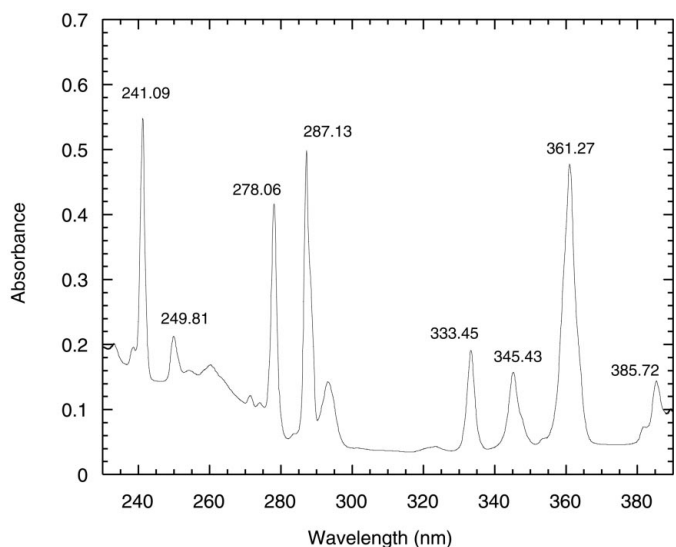


Figure 5 Holmium oxide absorbance spectrum measured on CD12 for wavelength calibration.

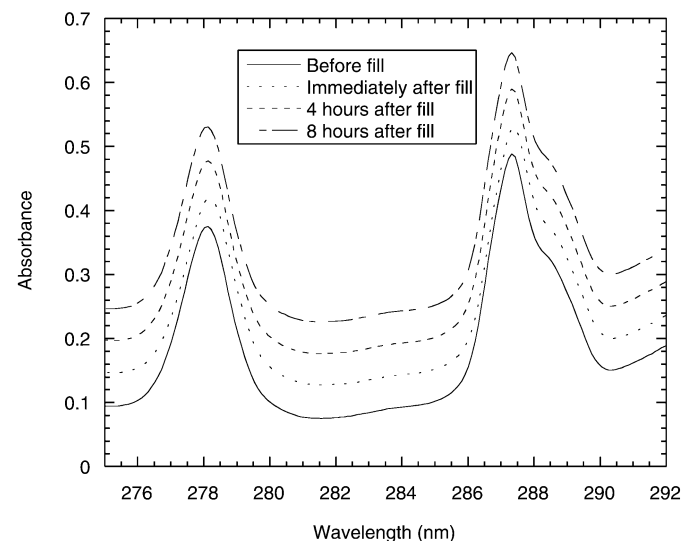


Figure 6 Series of holmium oxide absorbance spectra showing wavelength calibration stability of CD12. Curves are vertically displaced for clarity.

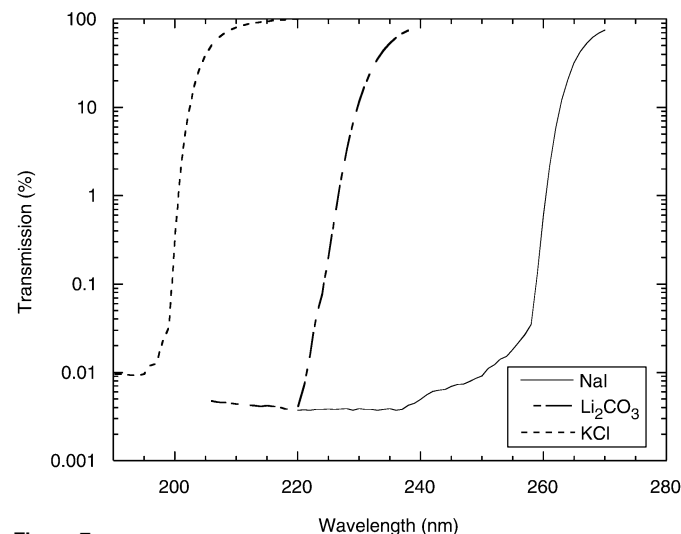


Figure 7 Transmission of standard salt solutions recorded on CD12 to measure levels of polychromatic stray light.

around 94%, with a maximum drift of 2% which is acceptable for the PEM (see below). Polarization stability is important as any drift in polarization leads to drifts in CD background. The CD background stability was measured by recording a series of CD spectra with no sample present. The apparatus was calibrated using a solution of (1*s*)-(+)-10-camphorsulphonic acid, and differences between successive scans determined as delta epsilon equivalent. These data (not shown) have shown maximum drifts in CD backgrounds of 0.05 delta epsilon per hour, confirming the stability of polarization. The above polarization data were obtained with the beam-defining baffles in the fully open position. Small increases in linear polarization (up to 97%) were obtained when the baffles were used to mask the upper and lower parts of the beam, but with consequent reduction in photon flux. Polarization was also stable with wavelength between 190 and 280 nm, with some reduction in overall degree of polarization at longer wavelengths. Measurements at lower wavelengths were not possible because of the wavelength cut-off of the polarization analyser's optical elements.

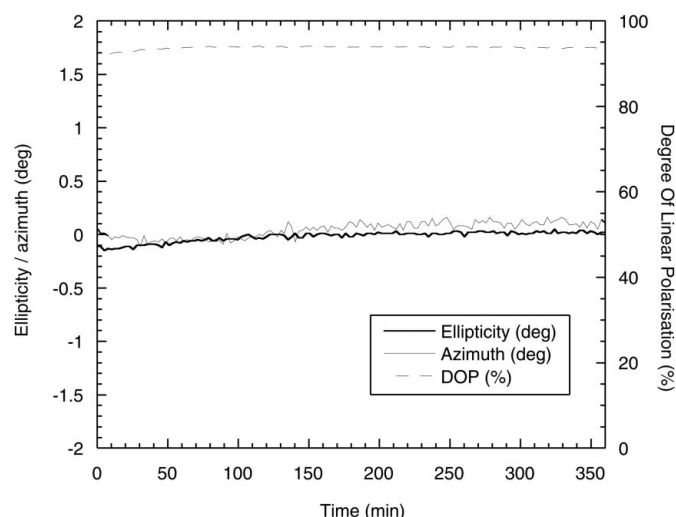


Figure 8
Measurement of CD12 polarization parameters, recorded over a 6 h period.

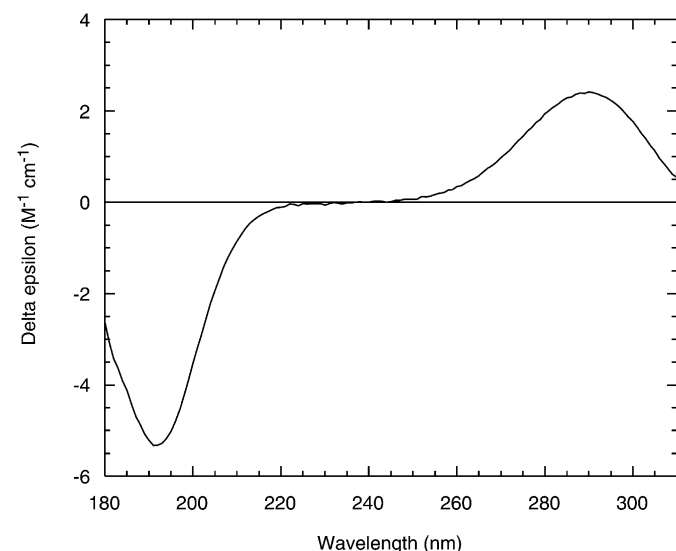


Figure 9
CD spectrum of (1*s*)-(+)-10-camphorsulphonic acid recorded on CD12.

4. Circular dichroism test measurements

4.1. Steady-state measurements

Fig. 9 shows a CD spectrum of 10 mg ml⁻¹ (1*s*)-(+)-10-camphorsulphonic acid (CSA) obtained on CD12, using a 0.1 mm-pathlength spectrosil cell (Hellma). The data were collected in 0.5 nm wavelength increments, with a counting time of 3 s per point. CSA is commonly used as a ellipticity calibration standard for CD instruments because of its two CD band maxima at 192.5 and 290.5 nm (Venyaninov & Yang, 1996). The value reported for the ratio of the two bands varies in the literature from 2.0 (Chen & Yang, 1977) to 2.2 (Gregoire & Loret, 1996), with the general consensus being around 2.1 (Johnson, 1996). We observe a ratio of 2.2 on CD12, at the upper end of the reported range. Low ratios are often the result of low light levels at short wavelengths and high contributions from stray light. The relatively high ratio of 2.2 observed on CD12 may be caused by the strong photon fluxes reaching the detector and low stray light contamination at this wavelength. Also, the slightly reduced degree of polarization observed at 290 nm may result in some suppression of the long-wavelength CSA band, increasing the ratio. However, spectra of proteins in the wavelength range between 160 and 260 nm reported in the following sections are consistent with published data, indicating that the degree of linear polarization of the beamline is appropriate for conversion to circularly polarized light by the PEM.

Fig. 10 shows the SRCD spectrum of myoglobin, recorded on CD12. Protein concentration was 10 mg ml⁻¹ and there was no smoothing routine employed. The spectrum from 260 to 180 nm was recorded in a 0.01 mm-pathlength cell, myoglobin was dissolved in water, and three scans were averaged, giving a total integration time of 3 s per point, with a wavelength step of 0.5 nm. The spectral bandwidth was 0.5 nm. Spectra from 200 to 160 nm were obtained using a cell consisting of two flat calcium fluoride plates (Crystran), sandwiched together to give a pathlength of approximately 1 µm. Myoglobin was dissolved in deuterium oxide, and ten scans averaged giving a total integration time of 10 s per point. As the pathlength was not known, these spectra were scaled to give the same CD intensity at 190 nm as those from the 0.01 mm cell. The spectra were then spliced together to produce the spectrum shown in Fig. 10. The inset shows the subtraction of the overlapping parts of the CD spectra taken in

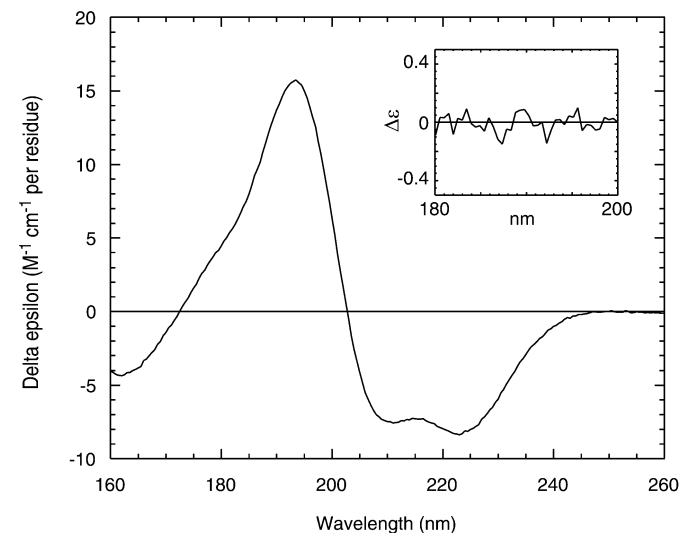


Figure 10
SRCD spectrum of a 10 mg ml⁻¹ myoglobin solution, recorded on CD12. The inset shows the difference between the spectra of myoglobin in H₂O and D₂O, over the wavelength range where the spectra were recorded in both solvents.

water and D₂O, indicating the similarity in spectral shape for the protein in the two solvents. The myoglobin spectrum is the same as those previously published over the wavelength range from 170 to 260 nm, with a shoulder at around 175 nm (Toumadje *et al.*, 1992). We also observe evidence of a CD minimum just above the wavelength cut-off of 160 nm.

We have also measured the CD spectrum of myoglobin dissolved in hexafluoro-2-propanol. This solvent transmits light at shorter wavelengths than water. Spectra were recorded of 10 mg ml⁻¹ myoglobin in hexafluoro-2-propanol in a 0.01 mm-pathlength spectrocell, from 260 to 170 nm, and as a thin film between two calcium fluoride plates, from 200 to 140 nm. The pathlength of the film was determined by comparison of the amplitudes of the CD maximum at 193 nm. After buffer subtraction and scaling, the spectra were joined, producing the spectrum shown in Fig. 11. The change in ratio between the 207 and 222 nm CD minima, compared with that obtained in water, indicates that some solvent-dependent protein structural changes have occurred. However, the spectrum still shows the char-

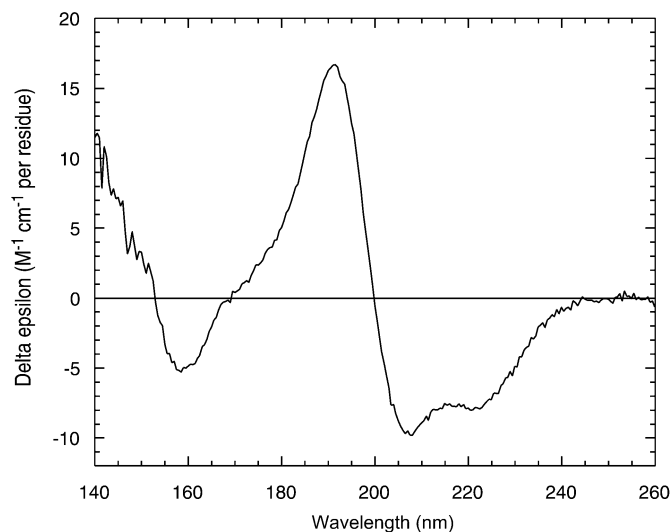


Figure 11
VUV CD spectrum of 10 mg ml⁻¹ myoglobin in hexafluoro-2-propanol.

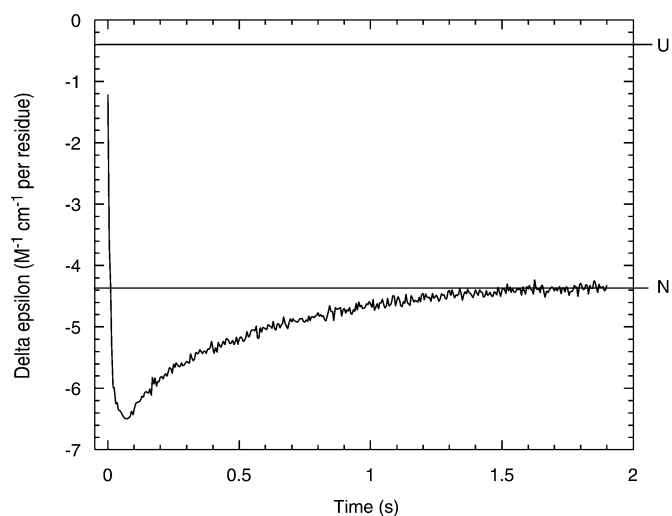


Figure 12
Folding of lysozyme monitored by stopped-flow SRCD at 222 nm on CD12. U and N indicate the CD amplitude for unfolded protein and for the native state, respectively.

acteristic shape for a helical protein. The spectrum is also consistent with those reported for helical polypeptides in the VUV (Johnson & Tinoco, 1972).

4.2. Time-resolved measurements

The suitability of CD12 for stopped-flow measurements was confirmed by measuring the refolding of lysozyme from guanidinium hydrochloride. The folding of this protein has been extensively investigated, CD measurements at 222 nm showing an initial fast overshoot in CD amplitude, followed by a slower return to the ellipticity of the native protein (Radford *et al.*, 1992). Fig. 12 shows stopped-flow CD data on lysozyme folding recorded on CD12. Data were recorded using a commercially available data-acquisition system (Applied Photophysics Ltd), with a specially constructed stopped-flow apparatus. The cell pathlength was 0.5 mm and the dead-time was 0.4 ms. A 1.0 mg ml⁻¹ solution of lysozyme in 6.0 M guanidinium hydrochloride was diluted at a mixing ratio of 1:10 with 20 mM sodium acetate, pH 5.0. Data were recorded at 222 nm with a time resolution of 0.5 ms. The data shown were obtained from a single protein shot of 10 µl total volume.

Folding kinetics are as previously reported (Radford *et al.*, 1992) although the CD signal at time zero is closer to the value for unfolded protein than previously reported, because of the shorter dead-time of our stopped-flow apparatus.

4.3. Radiation damage

The photon fluxes from CD12 are unprecedented for the measurement of CD spectra. To investigate the effect of radiation dose on a protein, CD spectra were continually recorded from a sample of myoglobin. The protein was dissolved in water at a concentration of 10 mg ml⁻¹, and loaded into a 0.01 mm-pathlength spectrocell demountable cell (Hellma). Spectra were collected at 4 min intervals, with a spectral resolution of 1 nm, wavelength increment of 0.5 nm, and integration time of 1 s per point, over a wavelength range from 260 to 170 nm. The scan time was 3 min and the residual time was taken up in resetting the monochromator to 260 nm before restarting its scanning routine. The buffer-subtracted spectra are shown in Fig. 13. The spectra show an increasing degradation of the amplitude of all CD features with beam exposure indicating struc-

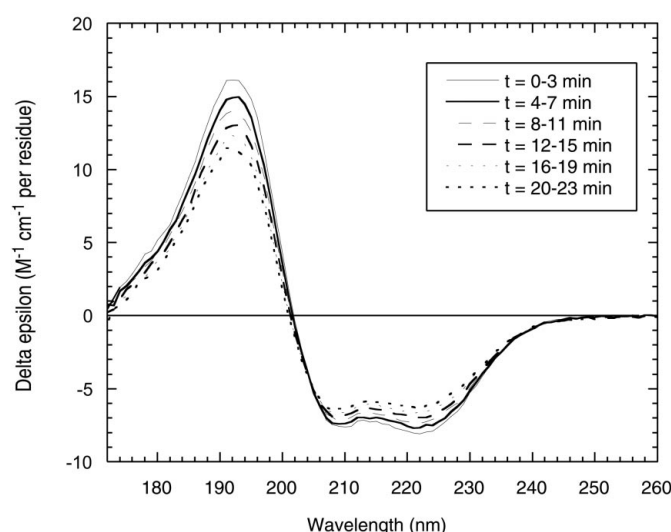


Figure 13
Series of CD spectra of the same sample of myoglobin, scanned from 260 to 170 nm, recorded at 4 min intervals.

tural damage to the protein. Further work will be required to show whether the changes to the CD spectrum arise from a general loss of protein signal caused by aggregation and precipitation of the protein or from the loss in the dominant helical content of the myoglobin structure. It has been reported that broadband UVC radiation with an accumulated dose of around 2 kJ m^{-2} begins to reduce the activity of, for example, lysozyme, probably through amino acid side-chain reactions (Durchschlag *et al.*, 2003). At wavelengths shorter than 185 nm, water radiolysis increasingly occurs (Laszlo & Dombi, 2002) and this must result in free-radical damage to the protein, again with consequential changes to the protein structure and hence the CD spectrum. A 4 min scan on CD12 would give a typical radiation dose of around 2.5 kJ m^{-2} , therefore significant radiation damage would be expected with repeat scanning. The shape of the CD spectrum accumulated during the first 3 min scan was, however, identical to a spectrum undertaken at an integrated dose four orders of magnitude lower, indicating that the protein suffered little radiation damage during the first scan.

The effects of radiation damage can be minimized by careful experimental design. Scanning should proceed from high to low wavelength. In particular, if lengthy data collection is required for good signal-to-noise ratios, a series of rapid scans, renewing the sample each time, is preferable. For most measurements the high flux of the CD12 beamline allows the collection of good signal-to-noise data in a single rapid scan, thus avoiding the effects of radiation damage.

5. Discussion

The data shown above demonstrate that CD12 has achieved its design specification. The photon flux is nearly five orders of magnitude greater than that of conventional instruments at 200 nm, and this advantage becomes even more significant in the VUV. The high photon flux, combined with the stability, polarization and resolution characteristics described above, makes CD12 an extremely effective facility for the measurement of CD.

The potential of the SRCD technique is demonstrated by the SRCD data presented. Fig. 10 shows that the range of the CD spectrum for proteins may be extended to wavelengths as short as 160 nm, with routine collection to a short-wavelength limit of approximately 175 nm. Fig. 11 demonstrates that absorption of the VUV radiation by the solvent is the limiting factor for samples in solution. Given a suitable solvent, spectra can be measured to at least 140 nm. The signal-to-noise ratios obtained are superior to those from conventional instruments when using similar data integration times. This will permit the collection of high-quality data from a large number of samples over a relatively short time. Good signal-to-noise ratios are essential for measurements that require high precision in secondary structure analysis. Fig. 14 shows the effect of the signal-to-noise ratio on precision of analysis. To approach a precision of 1%, RMS noise levels of less than $0.2\Delta\epsilon$ are required. These noise levels are easily attainable on CD12, but require the accumulation of many repeat scans with a conventional source. Examples of measurements that would require very high precision analysis are, for example, changes in enzyme active-site structure on the binding of ligands, or changes in chiral drug structure when they bind to their targets (Jones & Clarke, 2003).

The advantage of extending CD spectra to short wavelengths has been demonstrated, with significantly increased accuracy for protein secondary structure analysis (Jones & Clarke, 2003; Toumadje *et al.*, 1992). This is because of the additional information content contributed by the VUV part of the spectrum. Extending the

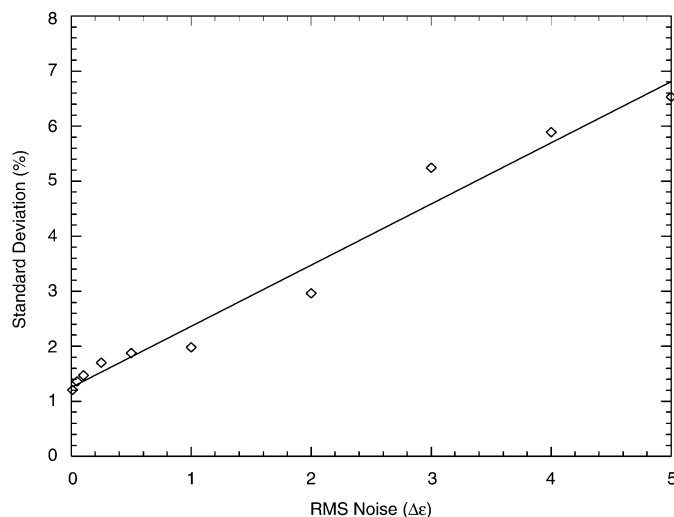


Figure 14

Effect of the signal-to-noise ratio on the precision of secondary structure analysis. Spectra were collected from three proteins (myoglobin, beta-lactoglobulin and papain), which differed widely in secondary structure, at a range of noise levels, and analysed for secondary structure content. Standard deviations of secondary structure content from CD analysis of five scans at each noise level are plotted *versus* RMS noise level.

spectra to this region should better enable the quantitation of minor secondary structure components, such as 3_{10} and polyproline II helix, and the various types of beta turns. However, successful measurement of these structure types will require significant extensions to the sets of CD basis spectra used for analysis. At present, these minor secondary structure components are insufficiently represented in the traditionally used basis sets to provide a meaningful analysis.

The value of SRCD for stopped-flow measurements has already been demonstrated (Jones & Clarke, 2003). This is because synchrotron radiation allows the collection of time-resolved spectra rather than single-wavelength data. This permits a more rigorous kinetic analysis based on the quantitation of secondary structure from time-resolved spectra rather than a single-wavelength CD signal. The high VUV flux of CD12 will extend the wavelength range for time-resolved CD, and allow the collection of data with good signal-to-noise ratios from smaller amounts of sample. This is important as protein studies will no longer be limited to those that can be obtained in large quantities.

The full benefits and potential of CD12 will only become apparent as data are collected over the next few years of operation. However, a number of developments are already planned. Firstly, the potential of SRCD for high-throughput screening has yet to be exploited. Automation of the station using microplate technology is feasible and would allow the collection of data from large numbers of samples alongside other high-throughput methods being presently developed, *e.g.* HTP protein crystallography. Array detectors for SRCD are currently under development (Manolopoulos *et al.*, 2003) to collect energy-dispersive spectra, reducing the time required to obtain a spectrum by orders of magnitude. Array detectors applied to time-resolved SRCD will reduce data-collection times significantly and reduce the sample weight requirements per experiment. However, the evidence presented here suggests that the photon fluxes achievable on the CD12 beamline represent a limit to the allowable radiation dose to which a protein can be exposed without employing free-radical scavengers or freezing methodologies.

For the present, large-aperture bending magnets are the preferred source for SRCD, because of their broad spectral output, which allows fast scanning and the use of energy-dispersive techniques. However, insertion devices should prove useful for specialized applications, such as fast time-resolved CD using the ellipsometric method (Goldbeck *et al.*, 1997). Fourth-generation light sources would appear to be particularly suitable for the measurement of VUV CD in the nanosecond and picosecond time domain where the gross effects of radiation damage may be avoided, and for specialized photon-hungry techniques, *e.g.* CD microscopy.

The authors would like to acknowledge and thank the BBRSC for part-funding the construction of CD12 through the centre of excellence in structural biology initiative (Grant No. 719/SB11261), and also CCLRC for the residual funding. We would also like to thank the Centre for Protein and Membrane Structure and Dynamics, especially the director, Professor B. Wallace, and the associate directors, Professor N. Price, Dr A. Rodger, Dr A. Drake and latterly Dr. R. Janes, for their support and advice during the construction project. Thanks are also due to the CCLRC CD12 project team led by Mr B. Todd.

References

- Berman, H. M., Westbrook, J., Feng, Z., Gilliland, G., Bhat, T. N., Weissig, H., Shindyalov, I. N. & Bourne, P. E. (2000). *Nucl. Acids Res.* **28**, 235–242.
- Chen, G. C. & Yang, J. T. (1977). *Anal. Lett.* **10**, 1195–1207.
- Clarke, D. T., Doig, A. J., Stapley, B. J. & Jones, G. R. (1999). *Proc. Nat. Acad. Sci. USA*, **96**, 7232–7237.
- Clarke, D. T. & Jones, G. R. (1999). *Biochemistry*, **38**, 10457–10462.
- Durchschlag, H., Hefferle, T. & Zipper, P. (2003). *Rad. Phys. Chem.* **67**, 479–486.
- Fasman, G. D. (1996). *Circular Dichroism and the Conformational Analysis of Biomolecules*. New York/London: Plenum Press.
- Frishman, D. & Argos, P. (1995). *Proteins Struct. Func. Genet.* **23**, 566–579.
- Goldbeck, R. A., KimShapiro, D. B. & Kliger, D. S. (1997). *Ann. Rev. Phys. Chem.* **48**, 453–479.
- Greenfield, N. J. (1996). *Anal. Biochem.* **235**, 1–10.
- Gregoire, C. J. & Loret, E. P. (1996). *J. Biol. Chem.* **271**, 22641–22646.
- Johnson, W. C. (1996). *Circular Dichroism and the Conformational Analysis of Biomolecules*, edited by G. Fasman, pp. 635–652. New York/London: Plenum Press.
- Johnson, W. C. & Tinoco, I. Jr (1972). *J. Am. Chem. Soc.* **94**, 4389–4390.
- Jones, G. R. & Clarke, D. T. (2003). *Faraday Discuss.* **126**. In the press.
- Jones, G. R. & Munro, I. H. (2000). *Structure and Dynamics of Biomolecules*, edited by E. Fanchon, pp. 305–337. Oxford University Press.
- Kemp, J. C. (1969). *J. Opt. Sci. Am.* **59**, 950–954.
- Kuwajima, K. (1996). *Circular Dichroism and the Conformational Analysis of Biomolecules*, edited by G. Fasman, pp. 159–182. New York/London: Plenum Press.
- Laszlo, Zs. & Dombi, A. (2002). *Chemosphere*, **46**, 491–494.
- Lobley, A., Whitmore, L. & Wallace, B. A. (2002). *Bioinformatics*, **18**, 211–212.
- Manolopoulos, S., Clarke, D. T., Derbyshire, G., Jones, G. R., Read, P. & Torbet, M. (2003). In preparation.
- Oakberg, T. C., Trunk, J. & Sutherland, J. C. (2000). *Proc. SPIE*, **4133**, 101–111.
- Radford, S. E., Dobson, C. M. & Evans, P. A. (1992). *Nature (London)*, **358**, 302–307.
- Rodger, A. & Nordén B. (1997). *Circular Dichroism and Linear Dichroism*. Oxford University Press.
- Snyder, P. A. & Rowe, E. M. (1980). *Nucl. Instrum. Methods*, **172**, 345–349.
- Stevens, E. S. (1996). *Circular Dichroism and the Conformational Analysis of Biomolecules*, edited by G. Fasman, pp. 501–530. New York/London: Plenum Press.
- Sutherland, J. C. (1996). *Circular Dichroism and the Conformational Analysis of Biomolecules*, edited by G. Fasman, pp. 599–633. New York/London: Plenum Press.
- Sutherland, J. C., Desmond, E. J. & Takacs, P. Z. (1980). *Nucl. Instrum. Methods*, **172**, 195–199.
- Sutherland, J. C., Emrick, A., France, L. L., Monteleone, D. C. & Trunk, J. (1992). *Biotechniques*, **13**, 588–590.
- Toumadje, A., Alcorn, S. W. & Johnson, W. C. (1992). *Anal. Biochem.* **200**, 321–331.
- Venjaminov, S. Y. & Yang, J. T. (1996). *Circular Dichroism and the Conformational Analysis of Biomolecules*, edited by G. Fasman, pp. 69–107. New York/London: Plenum Press.